PERGAMON

Quaternary Science Reviews 21 (2002) 295–305

QSR

Sea-level and deep water temperature changes derived from benthic foraminifera isotopic records

C. Waelbroeck[a,*], L. Labeyrie[a,b], E. Michel[a], J.C. Duplessy[a], J.F. McManus[c], K. Lambeck[d], E. Balbon[a], M. Labracherie[e]

[a] *Laboratoire des Sciences du Climat et de l'Environnement (LSCE), Domaine du CNRS, bât. 12, 91198 Gif-sur-Yvette, France*
[b] *Département des Sciences de la Terre, Université Paris-sud Orsay, bât. 504, 91104 Orsay, France*
[c] *Woods Hole Oceanographic Institution, Woods Hole, MA 02543, USA*
[d] *Research School of Earth Sciences, The Australian National University, Canberra 0200, Australia*
[e] *Département de Géologie et Océanographie, CNRS UMR 5805, Université de Bordeaux I, 33405 Talence, France*

Received 26 February 2001; accepted 4 September 2001

Abstract

We show that robust regressions can be established between relative sea-level (RSL) data and benthic foraminifera oxygen isotopic ratios from the North Atlantic and Equatorial Pacific Ocean over the last climatic cycle. We then apply these regressions to long benthic isotopic records retrieved at one North Atlantic and one Equatorial Pacific site to build a composite RSL curve, as well as the associated confidence interval, over the last four climatic cycles. Our proposed reconstruction of RSL is in good agreement with the sparse RSL data available prior to the last climatic cycle. We compute bottom water temperature changes at the two sites and at one Southern Indian Ocean site, taking into account potential variations in North Atlantic local deep water $\delta^{18}O$. Our results indicate that a Last Glacial Maximum (LGM) enrichment of the ocean mean oxygen isotopic ratio of 0.95‰ is the lowest value compatible with unfrozen deep waters in the Southern Indian Ocean if local deep water $\delta^{18}O$ did not increase during glacials with respect to present. Such a value of the LGM mean ocean isotopic enrichment would impose a maximum decrease in local bottom water $\delta^{18}O$ at the North Atlantic site of 0.30‰ during glacials.

1. Introduction

The amount of ice stored in the ice sheets is a key element of the climate system. The corresponding sea-level change record is also of major interest for paleoenvironmental studies. However, there is still no continuous record available over several climatic cycles. Records of sea-level change based on corals and other evidences are limited mainly to the period after the Last Glacial Maximum (LGM) (e.g. Fairbanks, 1989; Bard et al., 1990a, b, 1996; Chappell and Polach, 1991; Yokoyama et al., 2000; Hanebuth et al., 2000) and for earlier periods the record consists mostly of a few isolated points corresponding approximately to relative highstands (Chappell and Shackleton, 1986; Chappell et al., 1996; Lambeck and Chappell, 2001). Rohling et al. (1998) estimated the magnitude of sea-level low stands from records of extreme high-salinity conditions in the Red Sea. Sea level has also been inferred from the oxygen isotopic ratio measured on the calcite shells of benthic foraminifera. The shell $^{18}O/^{16}O$ ratio is a function of both the isotopic composition and the temperature of the water in which the foraminifera develops. Therefore, assuming that deep water temperature does not vary too much over time, the benthic $^{18}O/^{16}O$ ratio ($\delta^{18}O_b$, expressed in ‰ versus PDB, where PDB is the Chicago PDB-1 standard, Pee Dee Belemnite) can be used as a first order proxy for global ice volume. However, benthic curves do not match sea-level estimates based on fossil coral reef terraces. Chappell and Shackleton (1986) and Shackleton (1987) interpreted this mismatch as the result of deep water temperature changes and concluded that deep waters in the Pacific Ocean were about 1.5°C cooler during glacial times than today. Labeyrie et al. (1987) inferred sea level using benthic isotopic records from regions where changes in deep water

*Corresponding author. Tel.: +33-1-69-82-43-27; fax: +33-1-69-82-35-68.
E-mail address: claire.waelbroeck@lsce.cnrs-gif.fr (C. Waelbroeck).

0277-3791/02/$ - see front matter
PII: S0277-3791(01)00101-9

temperature were thought to be minimal, i.e., the Norwegian Sea during stages 1, 4 and 5, and the Pacific Ocean during stages 2 and 3.

Deriving a sea-level record from $\delta^{18}O_b$ data is complicated, however, not only due to variations in deep water temperature, but also due to possible temporal variation in the isotopic composition of the melted ice (Clarke et al., this volume) and changes in local deep water $\delta^{18}O_b$ that are not related to sea-level change (Rohling and Bigg, 1998). Currently, the North Atlantic (N. Atl.) Ocean is the location of active deep water formation, as warm and saline surface waters reach high latitudes where their density increases by cooling through intense heat exchange with the atmosphere. This cold bottom water mixes with warm and saline N. Atl. intermediate water while overflowing the Denmark and Faeroe sills. This gives relatively warm (2°C) and saline (> 34.9 practical salinity units) N. Atl. deep waters (NADW) with a water isotopic composition, $\delta^{18}O_w$, that is about 0.25‰ higher than the global mean (Ostlund et al., 1987). In contrast, deep waters formed around Antarctica are colder (<0°C), less saline (<34.7 p.s.u.), and of low $\delta^{18}O_w$ (about 0.2‰ lower than the global mean). The situation in the N. Atl. was likely very different during the LGM: the mean position of the polar front shifted south of the Denmark and Faeroe sills, and the deep water formation and thermohaline circulation apparently slowed down (Curry et al., 1988; Boyle, 1988; Duplessy et al., 1988a). Taking the Weddell Sea as a modern analog of the LGM N. Atl. (Labeyrie et al., 1987; Duplessy et al., 1988b) suggests that deep waters of very low-temperature and $\delta^{18}O_w$ could have formed near the margins of former circum-N. Atl. ice sheets. This would lead to larger temperature changes in the N. Atl. and reduced hydrological gradients between the N. Atl. and the other oceans during glacial periods (McManus et al., 1999a).

In the present study, we derive statistical sea-level transfer functions between high resolution $\delta^{18}O_b$ records and sea-level data based on corals and other evidences. We then reconstruct sea-level changes over four climatic cycles and deduce deep water temperature changes, taking into account potential variations in N. Atl. local deep water $\delta^{18}O$.

2. Material and methods

Within a given sediment core, the change in $\delta^{18}O_b$ with respect to present, $\Delta\delta^{18}O_b$, can be decomposed into three contributions: the change in deep water $\delta^{18}O$ related to sea-level and ice volume changes, $\Delta\delta_{ice\ vol}$ (global signal), the change in deep water $\delta^{18}O$ related to local $\delta^{18}O$ variations, $\Delta\delta_{local}$, and the impact of local deep water temperature changes on the oxygen fractionation between the foraminifera shell and water, $\Delta\delta_{temp}$.

$$\Delta\delta^{18}O_b = \Delta\delta^{18}O_w + \Delta\delta_{temp} = \Delta\delta_{ice\ vol} + \Delta\delta_{local} + \Delta\delta_{temp}. \quad (1)$$

Our purpose is to separate $\Delta\delta^{18}O_b$ into these three components in the N. Atl., the Southern and the Pacific Ocean, over the last four climatic cycles. The locations of the $\delta^{18}O_b$ records we use in this work are given in Table 1. N. Atl. cores NA 87-22 and NA 87-25 were retrieved at the same location as ODP core 980, the latter covering the last 500 kyr (McManus et al., 1999b). We patched NA 87-22 and NA 87-25 $\delta^{18}O_b$ records to form a high resolution record over the entire last climatic cycle. The Pacific Ocean data we use are from core V19-30 (Shackleton et al., 1983; Shackleton and Pisias, 1985) over stage 1–10, and from ODP core 677 data (Shackleton et al., 1990) over stage 10–12, whereas Southern Indian (S. Indian) Ocean core MD 94-101 provides a continuous record over the last four climatic cycles. Isotopic measurements on N. Atl. core NA 87-25 and S. Indian Ocean core MD 94-101 were performed at the LSCE on a Finnigan MAT251 mass-spectrometer. The mean external reproducibility (1σ) of carbonate standards is ± 0.05‰. $\delta^{18}O$ data are calibrated with respect to NBS19 (Hut, 1987; Coplen, 1988).

Table 1
Cores location and data references

Core	Ocean	Latitude	Longitude	Depth, (m)	Time span, (ka)	Benthic species analyzed	Reference
NA 87-22	North Atlantic	55°29′8N	14°41′7W	2161	0–75	*Cibicides wuellerstorfi*	Vidal et al., 1997
NA 87-25	North Atlantic	55°11′9N	14°44′9W	2320	75–140	*Cibicides wuellerstorfi*	Cortijo et al., 1994, 1999; H. Leclaire (LSCE)
ODP 980	North Atlantic	55°29′N	14°42′W	2179	0–500	*Cibicides wuellerstorfi*	McManus et al., 1999a, b
MD 94-101	Southern Indian Ocean	42°30′S	79°25′E	2920	0–430	*Cibicides wuellerstorfi*	Lemoine, 1998; Salvignac, 1998; this study
V 19-30	Equatorial Pacific Ocean	03°21′S	83°21′W	3091	0–340	*Uvigerina*	Shackleton et al., 1983; Shackleton and Pisias, 1985
ODP 677	Equatorial Pacific Ocean	01°12.44′N	83°44.22′W	3461	0–3000	*Uvigerina*	Shackleton et al., 1990

We dated all records >40 kyr BP by correlating with the SPECMAP reference series. Among these, the SPECMAP stack of Imbrie et al. (1984) covers the last 800 kyr with a relatively low resolution, the benthic stack of Martinson et al. (1987) has the highest time resolution over the last two climatic cycles, while the stack of Bassinot et al. (1994) has the highest resolution between 500 and 900 kyr BP. As the present study covers the last 430 kyr, we chose to correlate the long benthic records to the Martinson et al. (1987) stack over the last 280 kyr and to the stack of Imbrie et al. (1984) for the earlier part. The chronology of the last 40 kyr was derived from AMS ^{14}C dates, converted into calendar ages using the calibration curve of Stuiver et al. (1998). Numerous ^{14}C dates obtained on monospecific planktonic foraminifera samples selected in abundance peak over the top 450 cm of core NA 87-22 (Duplessy et al., 1992) and corrected for variable reservoir ages (Waelbroeck et al., 2001) provided a chronology of the last deglaciation at the N. Atl. site. Finally, we dated the $\delta^{18}O_b$ signal of Equatorial Pacific core V19-30 over the last 30 kyr by correlating with the $\delta^{18}O_b$ record of the neighboring ^{14}C dated core TR 163-31 (3°37′S, 83°58′W, 3210 m, Shackleton and Pisias, 1985). The average dating error is on the order of 500–800 yr for the last deglaciation and equal to that of the SPECMAP timescale (i.e., 1–4 kyr) prior to 40 kyr BP. All correlations were performed using the AnalySeries software (Paillard et al., 1996).

2.1. Transfer function between sea level and benthic $\delta^{18}O$

In comparing relative sea-level (RSL) estimates based on corals and other evidences (full references given in the caption of Fig. 1) with N. Atl. high resolution NA 87-22 + NA 87-25 and Pacific V19-30 $\delta^{18}O_b$ records over the last climatic cycle (Fig. 1), one identifies at each site two distinct regimes, corresponding to the last deglaciation on one hand, and to the progression from the last interglacial into the LGM on the other hand (Fig. 2). Note that, rather than RSL, which varies from location to location because of glacio-hydro-isostatic effects, eustatic or ice-volume equivalent sea level (ESL) should be used. However, because the two are approximately

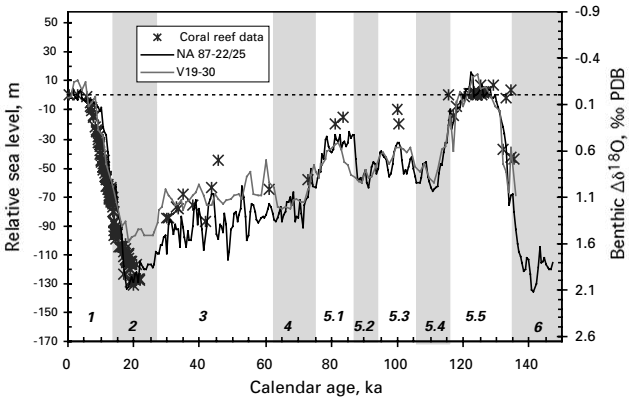

Fig. 1. Left axis: U-Th dated RSL estimates based on corals and other evidences (Bard et al., 1990a, b, 1996; Stein et al., 1993; Zhu et al., 1993; Gallup et al., 1994; Stirling et al., 1995; Chappell et al., 1996; Hanebuth et al., 2000; Yokoyama et al., 2000). Yokoyama's (2000) equivalent sea-level estimates have been converted into approximate RSL by subtracting 10 m. Right axis: North Atlantic patch of NA 87-22 and NA 87-25 $\delta^{18}O_b$ relative to the modern $\delta^{18}O_b$ value (3.32‰ PDB), and Pacific core V19-30 $\delta^{18}O_b$ relative to the modern value (3.45‰ PDB), both versus calibrated ^{14}C ages until 40 kyr BP, and versus the SPECMAP time scale beyond (see Table 1 for cores location and references). Note that the SPECMAP time scale has been adjusted to be consistent with the U-Th dated RSL data at the transition between stages 6 and 5. *Cibicides w.* $\delta^{18}O_b$ has been corrected by +0.64‰ to account for the difference in fractionation between this species and *Uvigerina* (Duplessy et al., 1984).

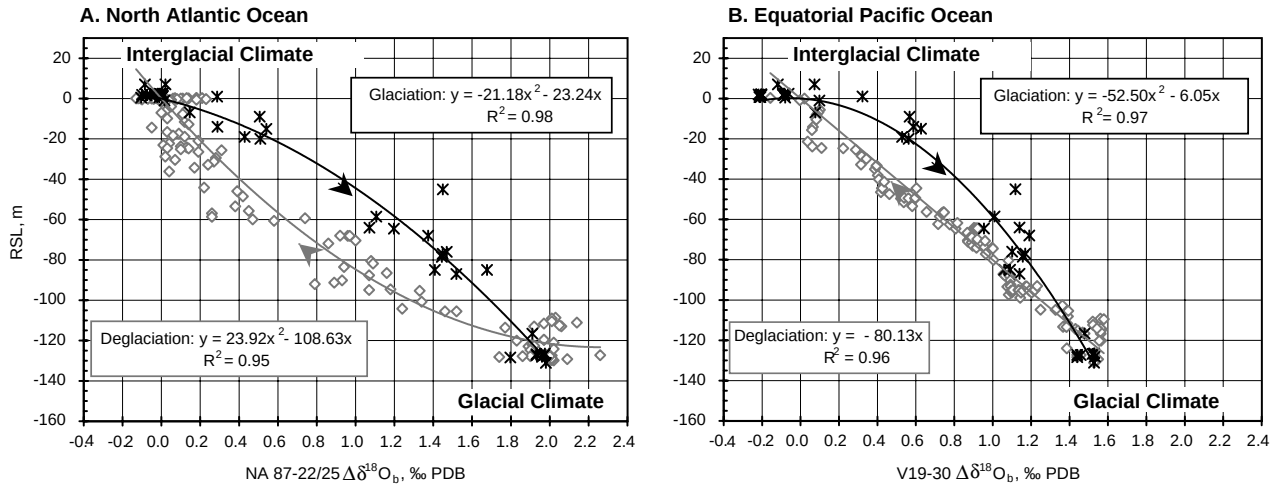

Fig. 2. (A) Open gray diamonds: RSL estimates (resampled) versus NA 87-22 $\Delta\delta^{18}O_b$ measurements over the last deglaciation (last 22 kyr). Crosses: estimated RSL versus NA 87-22/25 $\Delta\delta^{18}O_b$ (resampled) over the glaciation (129–19.5 kyr BP). (B) Same as in A, but for the Equatorial Pacific core V19-30.

proportional to each other for sites far from the former ice sheets, we have used for convenience RSL estimates.

The glaciation regime (from 129 to 19.5 kyr BP) is characterized by a regression of the second order, both in the N. Atl. and Pacific Oceans: $\Delta\delta^{18}O_b$ increased faster than RSL at the beginning of the glaciation, and then progressively more slowly until the ice sheets reached their maximum size. In other words, the rate of buildup of continental ice sheets appears to have been slower than the rate of decrease in local deep water temperature or increase in local deep water $\delta^{18}O$ at the beginning of the glaciation. On the contrary, after $\Delta\delta^{18}O_b$ had increased by about one third of the total interglacial–glacial amplitude, that is, during the period covering stages 4–2, the local deep water temperature decrease or $\delta^{18}O$ increase slowed down with respect to ice sheet buildup. This picture is consistent with ice sheets exhibiting a longer response time to climatic forcings than local deep water temperature and $\delta^{18}O$, which reflect changes in surface hydrology and/or ocean circulation.

During the last deglaciation, the general shape of the regression linking $\Delta\delta^{18}O_b$ to RSL is different at the N. Atl. and Pacific sites (Fig. 2). In the N. Atl., as for the glaciation regime, local deep water temperature and $\delta^{18}O$ change more rapidly than RSL at first and then slow down, yielding a quadratic regression. In contrast, the regression between RSL and Pacific $\Delta\delta^{18}O_b$ is not significantly different from a linear one and the increase in Pacific deep water temperature appears to be roughly in phase with sea-level rise.

The N. Atl. site is indeed located in a very sensitive area with respect to changes in the NADW rate of formation: whereas this site is within the core of NADW at present, it was at least partly under the influence of deep waters of southern origin during glacials (Duplessy et al., 1988a; Sarnthein et al., 1994). Therefore, this record contains a strong imprint of changes in water temperature, salinity and deep water ventilation. Conversely, the Equatorial Pacific site is located far from deep water formation areas, so that the water mass bathing this site is comparatively well mixed and more representative of the mean ocean water state than the water at the N. Atl. site (Duplessy et al., 1980). In short, the N. Atl. data are at higher resolution than the Pacific data but contain a very large local temperature signal (total N. Atl. $\Delta\delta^{18}O_b$ range $\approx 2‰$), whereas the Pacific $\delta^{18}O_b$ data are at lower resolution but are largely driven by RSL changes (total Pacific $\Delta\delta^{18}O_b$ range $\approx 1.5‰$).

We performed a sensitivity analysis to test the robustness of these glaciation and deglaciation regressions with respect to the interpolation procedure and dating. For the last deglaciation, one has the choice of either computing $\Delta\delta^{18}O_b$ at the ages of the dated coral RSL data, or computing RSL at ages corresponding to $\Delta\delta^{18}O_b$ measurements. The regression based on resampling $\Delta\delta^{18}O_b$ is very similar to that based on resampling RSL, yielding a maximum uncertainty on RSL of ± 4 m. In order to test the impact of dating errors, we successively subtracted and added an error of 500–800 yr to the nominal time scale of Fig. 1 during the last 30 kyr, accounting for the uncertainty in reservoir age correction (Waelbroeck et al., 2001), and of 1000 yr before. All the corresponding regression curves have determination coefficients >0.91. This exercise allowed us to determine that the maximum error on reconstructed RSL due to the dating uncertainty along the entire last climatic cycle and to the interpolation procedure during the last deglaciation is ± 8 m. Since the root mean square error of the deglaciation and glaciation regressions is 3/4/10 m, the total resulting error is $<\pm 13$ m.

3. Sea-level reconstruction

We applied the N. Atl. regressions to the ODP 980 $\Delta\delta^{18}O_b$ record, and the Pacific regressions to the V19-30/ODP 677 $\Delta\delta^{18}O_b$ record to reconstruct RSL over the last four climatic cycles (Fig. 3). The overall agreement between the two curves is satisfactory.

However, RSL derived from N. Atl. $\Delta\delta^{18}O_b$ data is 20–30 m higher than RSL based on Pacific $\Delta\delta^{18}O_b$ in portions of stages 4, 6 and 8. Those sections of the records correspond to RSL values between 90 and 120 m. Because there is no data in this RSL range, the N. Atl. and Pacific glaciation regressions are not properly constrained over this range. Therefore, the discrepancy between RSL derived from N. Atl. and from Pacific

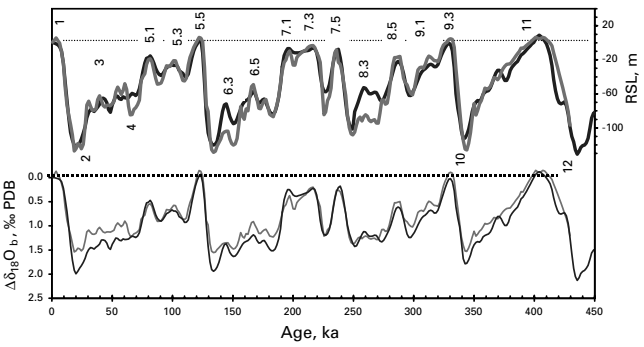

Fig. 3. Right axis: RSL reconstructed by application of the N. Atl. regressions to the N. Atl. $\Delta\delta^{18}O_b$ long record (black line) and of the Pacific regressions to the Pacific long $\delta^{18}O_b$ record (gray line). The numbers denote marine isotopic stages. Left axis: long N. Atl. (black line) and Pacific (gray line) $\Delta\delta^{18}O_b$ records (see Table 1 for cores location and references). The last climatic cycle of ODP 980 $\delta^{18}O_b$ record has been replaced by the higher resolution data from cores NA 87-22 and 87-25. In order to ensure the continuity between the V 19-30 and ODP 677 $\delta^{18}O_b$ records, 0.12‰ has been subtracted from the ODP677 $\delta^{18}O_b$ values. All records have been smoothed (7 points).

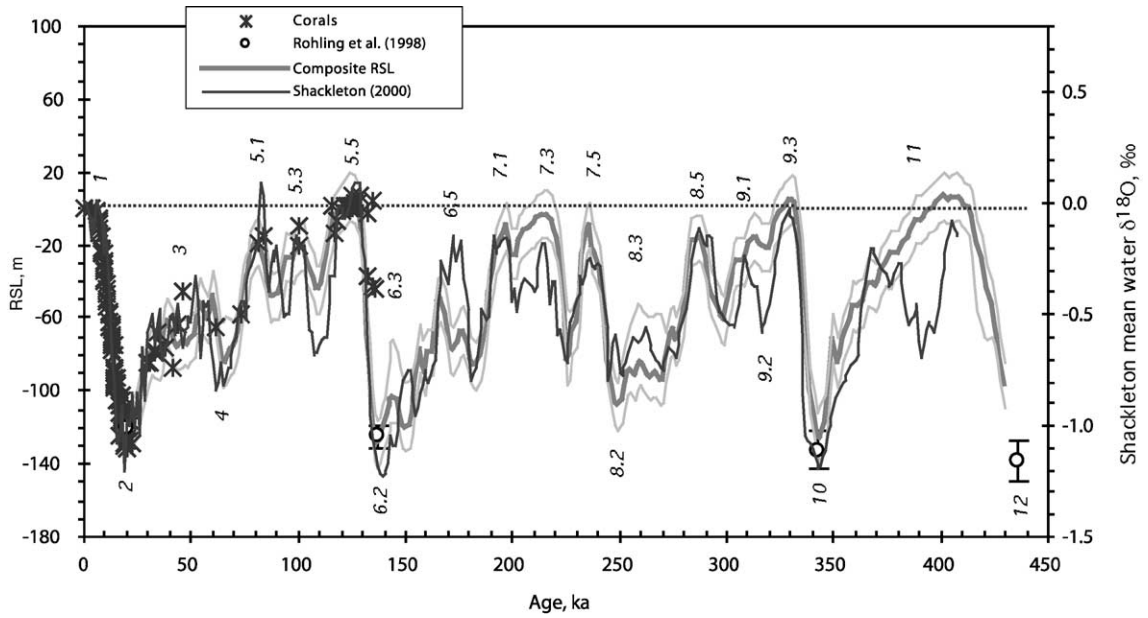

Fig. 4. Left axis: Composite RSL curve (bold gray line) and associated confidence interval (thin gray lines). Crosses: coral reef RSL data as in Fig. 1. Empty circles: RSL low stands estimated by Rohling et al. (1998). Right axis: variations in mean ocean water $\delta^{18}O$ derived by Shackleton (2000) from atmospheric $\delta^{18}O$ (black line).

$\Delta\delta^{18}O_b$ might result from the indeterminate shape of the N. Atl. and Pacific glaciation regressions in this RSL range. The difference between N. Atl. and Pacific reconstructions provides thus a measure of the uncertainty resulting from the method, given the present RSL data set. Note that there is likely to be a large error on the N. Atl. based RSL reconstruction during stage 12 because N. Atl. $\Delta\delta^{18}O_b$ increases beyond the calibration range over that period.

In order to facilitate the analysis of the results, we built a composite RSL curve over the last 432 kyr out of the most reliable sections of each reconstruction (Fig. 4). Because the Pacific $\Delta\delta^{18}O_b$ record is more representative of the mean ocean, we consider that the RSL reconstruction based on Pacific data is more reliable in general. The composite RSL curve is thus based on Pacific data over most of the studied time span (38–432 kyr BP). We used RSL derived from N. Atl. data over the last deglaciation to take advantage of the well-dated high-resolution record of core NA 87–22. We assume that the error on the composite reconstructed RSL is delimited by the N. Atl. and Pacific curves, and equal or larger than the uncertainty of ± 13 m due to the definition of the regressions.

4. Deep water temperature changes

In order to be able to compute local deep water temperature and $\delta^{18}O$ changes, meters of RSL change have to be translated into ‰ of mean ocean $\delta^{18}O_w$ change, $\Delta\delta_{ice\ vol}$ (Eq. (1)). Numerous uncertainties remain regarding the relationship linking RSL changes to $\Delta\delta_{ice\ vol}$.

First, as noted briefly above, RSL measured at any one locality does not relate directly to ice volume because of glacio-hydro-isostatic effects. However, for locations far from the former ice sheets these effects are relatively small and can be corrected for with adequate precision. Accounting for these corrections, sea-level data from Huon Peninsula (New Guinea) and Bonaparte Gulf (North Australia) and other localities have been recently converted into estimates of ice volume, or the ice-volume ESL, over the last climatic cycle (Yokoyama, 2000; Lambeck and Chappell, 2001; Lambeck et al., this volume). This results in many more data points being available for calculating the correlation, particularly for the periods when sea levels were in between their extreme values in the pre-LGM period. We attempted to apply the above approach to this new data set but obtained a much larger dispersion about the glaciation regressions than before (root mean square error of prediction of 15–18 m instead of 7–10 m). This suggests that the correlation between sea level and $\delta^{18}O_b$ may be more complex than assumed in the initial analysis and that this complexity is emphasized by the sampling characteristics of the sea-level estimates. For example, the sea-level estimates derived from the Huon coral data, because of the rapid tectonic uplift, are associated with times of relatively fast sea-level rise. The data correspond therefore, to non-representative sampling of the sea-level variations,

compared to the $\delta^{18}O_b$ records used which are of lower time resolution and which have been subjected to a greater degree of smoothing. Moreover, the dating of the marine series is largely uncertain prior to 40 kyr BP and it is necessary to bring the time scales of the two data sets into concordance. For a very high-resolution very well-dated $\delta^{18}O_b$ record, we would anticipate an improved match with the light $\delta^{18}O_b$ peaks but for the present we have to content ourselves with the available $\delta^{18}O_b$ records.

Second, the LGM $\Delta\delta_{ice\ vol}$ value is not firmly known. Measurements of sediment pore water $\delta^{18}O$ indicate that the global mean $\delta^{18}O_w$ enrichment during the LGM was 1 ± 0.1‰ (Schrag et al., 1996), whereas other studies, based on indirect evidence suggest a value between 0.87 and 1.3‰ (Labeyrie et al., 1987; Fairbanks, 1989; Duplessy et al., this volume). We start by assuming that an RSL drop of 130 m (Yokoyama et al., 2000) corresponds to a global mean $\delta^{18}O_w$ enrichment of 1.1‰ and then discuss the implications of this assumption in the light of our results.

Third, the exact shape of the relationship between RSL changes and variations in $\Delta\delta_{ice\ vol}$ is not known. It is usually assumed that RSL can be linearly linked to $\Delta\delta_{ice\ vol}$ by multiplication by a constant factor. However, this coefficient should vary in time, due to temporal variations in the isotopic composition of the stored ice (Mix and Ruddiman, 1984). The ice isotopic composition mainly depends on the temperature of precipitation formation above the ice sheet and on the water vapor trajectory (Lorius and Merlivat, 1977; Delaygue et al., 2000). Therefore, the ice that first accumulated in high-latitude polar ice sheets may have been isotopically lighter than the ice that accumulated at the end of the glaciation, when the northern ice sheets were reaching much further south. If this was the case, then this effect would induce quadratic regressions between $\delta^{18}O_b$ and RSL data during glaciation and deglaciation. Nevertheless, this effect is very small and does not explain the observed non-linearity (Chappell and Shackleton, 1986). We thus adopt here the simple hypothesis of a constant coefficient of 1.1‰/130 m.

Knowing $\Delta\delta_{ice\ vol}$, Eq. (1) yields the foraminifera isotopic change corresponding to local deep water temperature and $\delta^{18}O$ change, $\Delta\delta_{temp} + \Delta\delta_{local} \cdot \Delta\delta_{temp}$, the oxygen fractionation between foraminifera calcite and water, can be related to the water temperature through paleotemperature equations (Table 2). Several recent studies have proposed new equations for temperatures above 5°C (Bemis and Spero, 1998; Lynch-Stieglitz et al., 1999). However, using core-top *Cibicides wuellerstorfi* $\delta^{18}O$ data from sites that have current bottom temperatures <5°C, we verified that the commonly used paleotemperature equation of Shackleton (1974) provides the best fit with our data at low-temperatures (see Fig. 2 of Duplessy et al., this volume).

As the Pacific Ocean represents the largest ocean basin on the globe, we may assume that its $\delta^{18}O_w$ has always been close to the global mean $\delta^{18}O_w$, that is, Pacific Ocean deep water $\Delta\delta_{local}$ remained equal to zero. Therefore, the change in $\delta^{18}O_b$ due to temperature variations, $\Delta\delta_{temp}$, is simply given by the difference between $\Delta\delta^{18}O_b$ and $\Delta\delta_{ice\ vol}$ (Eq. (1)). With this assumption, the computed bottom water temperature at the Pacific site reaches a minimum value of about 0°C during glacials (Fig. 5A). Our Pacific deep water temperature reconstruction supports previous studies in which it was assumed that deep water cooling occurred entirely during the transition between stage 5.5 and 5.4 at the V19-30 site (Chappell and Shackleton, 1986; Labeyrie et al., 1987; Sowers et al., 1993).

We have no information on how $\Delta\delta_{local}$ evolved at the S. Indian site. However, the estimated modern local deep water $\delta^{18}O$ is extremely close to that of the global mean ocean (Table 2). Assuming S. Indian $\Delta\delta_{local} = 0$ as a first guess, the reconstructed bottom temperature during the LGM is -1°C. The bottom temperature at this site reaches a minimum of ~ -1.3 to -1.5°C during

Table 2
Holocene deep water hydrological conditions and isotopic data at the three long records sites

Ocean	Core	WOA 94		Eastimated modern $\delta^{18}O_w$ (‰ SMOW)[a]	Holocene $\delta^{18}O_b$ (‰ PDB)	Computed temperature[e] (°C)
		Temperature (°C)	Salinity (p.s.u.)			
North Atlantic	NA 97-22	3.50	34.95	0.246[b]	3.32	3.37
Southern Ocean	MD 94-101	1.67	34.73	0.005[c]	3.40	2.19
Pacific Ocean	V19-30	1.80	34.68	−0.002[d]	3.45	1.98

[a] SMOW is the Standard Mean Ocean Water: ‰ SMOW = ‰ PDB + 0.27‰.
[b] Regression on North Atlantic GEOSECS data (Ostlund et al., 1987) at all depths.
[c] Regression on Southern Indian Ocean GEOSECS data below 2500 m.
[d] Mean of Pacific GEOSECS data below 2000 m, the regression coefficient being too weak (0.005).
[e] Computed according to the paleotemperature equation of Shackleton (1974): $T = 16.9 - 4.38 \cdot (\delta^{18}O_b - \delta^{18}O_w + 0.27) + 0.1 \cdot (\delta^{18}O_b - \delta^{18}O_w + 0.27)^2$.

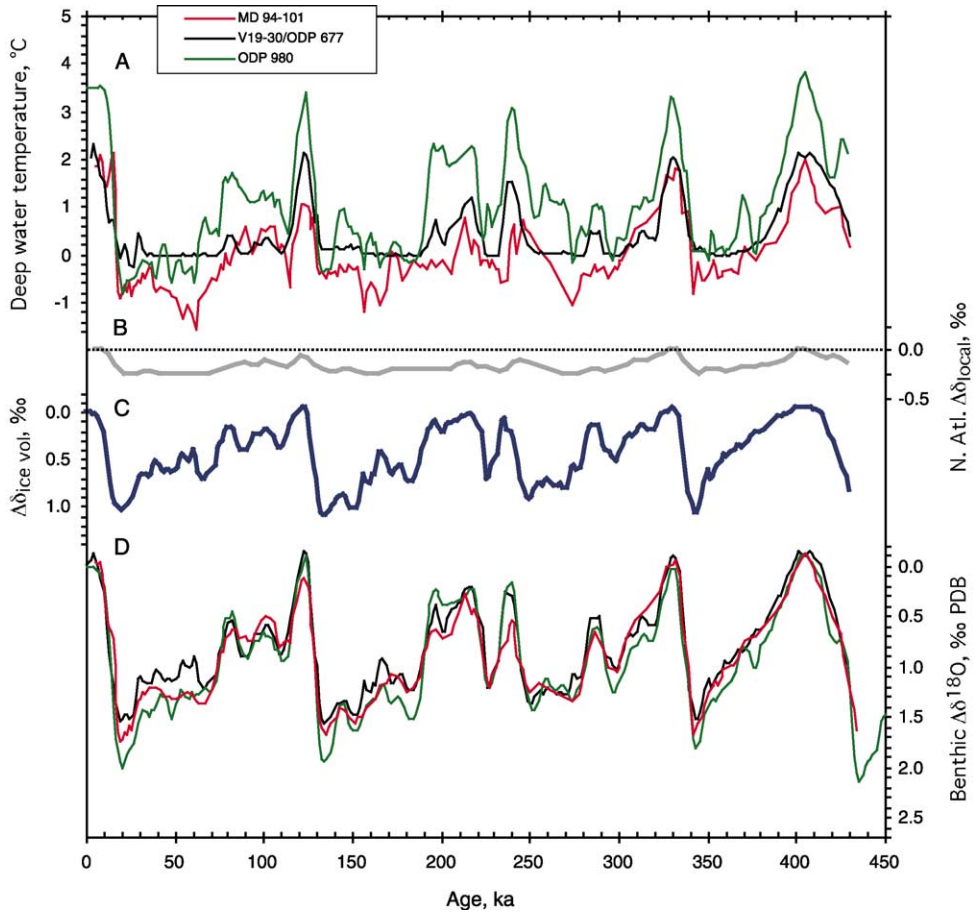

Fig. 5. (A) Computed bottom water temperature derived at the N. Atl., S. Indian and Pacific sites. (B) Modeled variations in N. Atl. local bottom water $\delta^{18}O$ with respect to present N. Atl. bottom water $\delta^{18}O$, $\Delta\delta_{local}$. (C) Reconstructed mean ocean water $\delta^{18}O$, $\Delta\delta_{icevol}$. (D) Smoothed long $\Delta\delta^{18}O_b$ records (same legend as in A).

stage 3. Nevertheless, this very low reconstructed temperature might be an artifact resulting from an erroneous temporary increase in RSL (i.e., lowerings in $\Delta\delta_{ice\ vol}$).

The situation in the N. Atl. is much more complex since N. Atl. $\Delta\delta_{local}$ likely varied between glacials and interglacials. The present-day deep water $\delta^{18}O$ at ODP site 980 is 0.25‰ higher than the deep water $\delta^{18}O$ at the Pacific and S. Indian sites (Table 2). In the following, we assume that N. Atl. $\Delta\delta_{local}$ decreases during glacials, as a result of the reduced input of warm and salty well ventilated NADW and enhanced northward penetration of colder, less saline and less ventilated deep waters of southern origin into the Atlantic Ocean basin. As NADW mixes with cold Antarctic bottom waters while flowing out of the Atlantic basin, warmer bottom temperatures at the S. Indian site indicate a larger NADW flow. We can thus use the reconstructed bottom water temperature at the S. Indian site as an index of the magnitude of the NADW flow. We propose a simple model, assuming that N. Atl. $\Delta\delta_{local}$ varies linearly from 0 to a lower limit, $-X$, when the S. Indian deep water temperature varies from temperatures warmer or equal to today ($\Delta\delta_{temp} \leqslant 0$) to glacial values ($\Delta\delta_{temp} \geqslant 0.65$) (Fig. 5B):

$$\begin{aligned} &\text{N. Atl. } \Delta\delta_{local} = 0 && \text{if S.I. } \Delta\delta_{temp} \leqslant 0 \\ &\text{N. Atl. } \Delta\delta_{local} = -X/0.65 \cdot \text{S.I. } \Delta\delta_{temp} && \text{if } 0 < \text{S.I. } \Delta\delta_{temp} \leqslant 0.65 \\ &\text{N. Atl. } \Delta\delta_{local} = -X && \text{if } 0.65 < \text{S.I. } \Delta\delta_{temp}. \end{aligned} \quad (2)$$

We take $X = 0.25$‰ as a first guess. This corresponds to the hypothetical situation of full glacials characterized by no $\delta^{18}O$ gradient between the N. Atl. Ocean and the other ocean basins. The change in N. Atl. $\Delta\delta^{18}O_b$ due to deep water temperature variations, $\Delta\delta_{temp}$, can then be easily computed (Eq. (1)), yielding a minimum temperature at the N. Atl. site of -0.8°C during stage 2 (Fig. 5A).

In the following section we focus our discussion on the LGM for which the reconstructed RSL is well constrained (within ± 13 m ≈ 0.12‰) and hence the

uncertainty on the bottom water reconstruction is minimal (i.e., about $\pm 0.5^{\circ}C$, as for the Levitus (1994) temperature data).

5. Discussion

5.1. Constraints on the LGM mean ocean isotopic enrichment and N. Atl. local deep water $\delta^{18}O$ change

A lower limit for bottom water temperature is constrained by the freezing point of sea water ($-1.9^{\circ}C$ at the sea surface). The in situ deep water minimum temperature is higher than at sea surface, due to the adiabatic warming that surface waters experience during sinking, leading to a lower limit of about $-1.8^{\circ}C$ at the N. Atl. site and of about $-1.75^{\circ}C$ at the S. Indian and Pacific sites. However, additional warming of descending water occurs during deep circulation, by mixing with warmer waters. Therefore, we consider that the extreme lower limit for bottom water temperature at our sites is $-1.5^{\circ}C$.

The bottom temperature reconstructed during the LGM is lowest at the S. Indian site (Fig. 5A). Assuming a $\Delta\delta_{ice\ vol}$ enrichment of 1.1‰ during the LGM and no change in S. Indian local deep water $\delta^{18}O$, the reconstructed bottom water temperature during stage 2 at the S. Indian site is $\sim -0.9^{\circ}C$. A lowering of the LGM $\Delta\delta_{ice\ vol}$ to 0.95‰ would yield LGM bottom water temperatures equal to the extreme lower limit of $-1.5^{\circ}C$ (Fig. 6). On the other hand, local deep water $\delta^{18}O$ could differ from the modern value if the amount of deep water formed around Antarctica changed. Present-day deep waters formed in the Weddell Sea have very low-temperature ($<0^{\circ}C$) and $\delta^{18}O$ (about 0.2‰ lower than the global mean). Therefore, a change in the quantity of deep water formed around Antarctica could lead to small variations in local deep water $\delta^{18}O$ at the S. Indian site. For instance, for an LGM $\Delta\delta_{ice\ vol}$ of 1.1‰, the extreme lower limit for bottom water temperature imposes a maximum decrease in local bottom water $\delta^{18}O$ at a S. Indian site of 0.15‰ (Fig. 6). Note that the LGM $\Delta\delta_{ice\ vol}$ could decrease below 0.95‰ if $\Delta\delta_{local}$ increased during glacials.

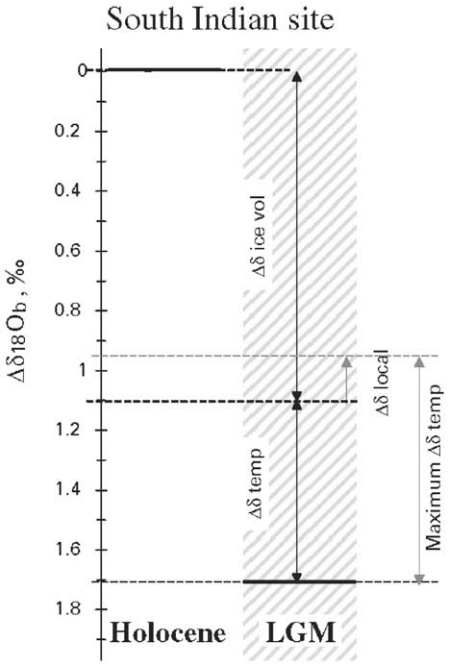

Fig. 6. Sketch of the Holocene-LGM shift in MD 94-101 $\Delta\delta^{18}O_b$ record (S. Indian site) indicating the partition between $\Delta\delta_{ice\ vol}$, $\Delta\delta_{local}$ and $\Delta\delta_{temp}$ and how changes in $\Delta\delta_{ice\ vol}$ or $\Delta\delta_{local}$ affect $\Delta\delta_{temp}$.

At the Equatorial Pacific site, the bottom temperature during stage 2 is $\sim 0^{\circ}C$ assuming no change in Pacific deep water $\delta^{18}O$. Lowering the LGM to 0.95‰ would yield bottom temperatures of $-0.5^{\circ}C$. We see that the temperature reconstruction at this site does not bring any further constraint on the minimum mean ocean isotopic enrichment compatible with an unfrozen ocean during the LGM.

At the N. Atl. site, the bottom water temperature during stage 2 is $-0.8^{\circ}C$ assuming $\Delta\delta_{ice\ vol} = 1.1‰$ and $\Delta\delta_{local} = -0.25‰$. Lowering the LGM $\Delta\delta_{ice\ vol}$ to 0.95‰ would bring bottom water temperature to $-1.3^{\circ}C$. Because the amplitude of the decrease in N. Atl. deep water $\delta^{18}O$ is not known, no further constraint on the minimum LGM $\Delta\delta_{ice\ vol}$ can be inferred from the N. Atl. temperature reconstruction. However, the maximum decrease in local deep water $\delta^{18}O$ compatible with unfrozen deep waters can be evaluated: taking an LGM $\Delta\delta_{ice\ vol}$ of 0.95‰, bottom water temperature reaches $-1.5^{\circ}C$ for a 0.3‰ decrease in local deep water $\delta^{18}O$.

5.2. Comparison of the reconstructed RSL with other data

Our composite RSL curve is, by construction, in excellent agreement with RSL data based on corals and other evidences over the last climatic cycle. Our results are in good agreement with the Rohling et al. (1998) estimates of sea-level lowstands over the last 400 kyr (Fig. 4), and with the few data on high sea-level stands derived from corals (Gallup et al., 1994; Bard et al., 1996). On the contrary, our reconstruction is significantly different from the RSL curve recently derived by Shackleton (2000) from the atmospheric $\delta^{18}O$ ($\delta^{18}O_{atm}$) recorded in the Vostok ice core. The discrepancy is especially large during stages 5.4, 6.5, 7.3, 7.5, 9.2 and 11 (Fig. 4). Data from coral reef terraces indicate that sea level was as high, or higher than today during stages 7.3, 7.5, 9.1 and 9.3 (Gallup et al., 1994; Bard et al., 1996). These data thus indicate that the RSL derived from $\delta^{18}O_{atm}$ (Shackleton, 2000) is at least 20 m too low during stages 7.3 and 7.5. Moreover, new geochemical data measured on a speleothem collected in Argentarola

cave at 19 m below present sea level show that whereas the sea level during stage 7.1 was between 19 and 12 m below present sea level, it was <19 m during stage 6.5 (Bard et al., 2000). This finding is in agreement with our proposed RSL reconstruction, but is in clear disagreement with the RSL derived by Shackleton (2000). Therefore, the present study appears to provide a reliable reconstruction of RSL over the last four climatic cycles, together with an estimate of the associated confidence interval. Note that our $\Delta\delta_{ice\ vol}$ curve is in good agreement with the mean ocean $\delta^{18}O$ curves proposed by Labeyrie et al. (1987) and Sowers et al. (1993).

6. Conclusion

We propose a continuous reconstruction of RSL that is compatible with available RSL data over the last four climatic cycles. This RSL reconstruction will have to be further validated with new RSL data derived from coral reef terraces or from other archives that are independent from benthic foraminifera isotopic ratios. Local deep water temperature and $\delta^{18}O$ estimates could also be validated if direct measurements of these quantities become available. Measurements of sediment pore water $\delta^{18}O$ indicate that the change in N. Atl. deep water $\delta^{18}O$ associated with the last deglaciation is about 0.8 ± 0.1‰, whereas the change in global mean ocean $\delta^{18}O$ is 1 ± 0.1‰ (Schrag et al., 1996). Accordingly, N. Atl. local deep water $\delta^{18}O$ decreased by 0.2 ± 0.1‰ during the LGM. These numbers are compatible with our results. Our estimate of the minimum possible change in global mean ocean $\delta^{18}O$ is 0.95‰ for no change in S. Indian local deep water $\delta^{18}O$. Such a value of the global mean ocean enrichment leads to a maximum decrease in the N. Atl. site local deep water $\delta^{18}O$ of 0.3‰ during the LGM. Concerning the validation of the deep water temperature reconstruction itself, Mg/Ca ratios in benthic foraminifera shells offer the potential to become an index of deep water temperature. Finally, another approach that should shed light on the validity of the hypotheses used in the present study is the modeling of ice sheet isotopic composition (Clarke et al., this volume). Potentially, if ice sheet growth, decay and isotopic composition can be correctly simulated, the change in mean ocean isotopic composition could be computed and directly compared with our global mean ocean $\delta^{18}O$ curve (Fig. 5C).

Acknowledgements

We thank T. van Weering for giving us access to core NA 87-25, and H. Leclaire for support in micropaleontology and for the study of core NA 87-25. We acknowledge B. Lecoat and J. Tessier for running isotopic measurements in Gif. We also thank M. Arnold and M. Paterne for ^{14}C measurements on core NA 87-22. F. Lemoine, M.E. Salvignac and G. Siani contributed to the sample preparation and measurements for core MD 94-101. The Marion-Dufresne cores have been collected under the responsibility of the IFRTP oceanic team directed by Y. Balut. This work has been supported by the CNRS, CEA and IFRTP, as well as by the French Programme National de la Dynamique du Climat. We thank E. Rohling and L. Stott for helpful reviews of the initial manuscript. This is contribution no. 0400 of the LSCE.

References

Bard, E., Hamelin, B., Fairbanks, R.G., 1990a. U-Th ages obtained by mass spectrometry in corals from Barbados: sea level during the past 130000 years. Nature 346, 456–458.

Bard, E., Hamelin, B., Fairbanks, R.G., Zindler, A., 1990b. Calibration of the ^{14}C timescale over the past 30000 years using mass spectrometric U-Th ages from Barbados corals. Nature 345, 405–410.

Bard, E., Hamelin, B., Arnold, M., Montaggioni, L., Cabioch, G., Faure, G., Rougerie, F., 1996. Deglacial sea-level record from Tahiti corals and the timing of global meltwater discharge. Nature 382, 241–244.

Bard, E., Antonioli, F., Rostek, F., Silenzi, S., Schrag, D.P., 2000. The penultimate glaciation as viewed from geochemical data measured in a submerged speleothem from Italy. EOS 81(19)(suppl.), S79.

Bassinot, F., Labeyrie, L., Vincent, E., Quidelleur, X., Shackleton, N., Lancelot, Y., 1994. The astronomical theory of climate and the age of the Brunhes-Matuyama magnetic reversal. Earth and Planetary Science Letters 126, 91–108.

Bemis, B.E., Spero, H.J., 1998. Reevaluation of the oxygen isotopic composition of planktonic foraminifera: experimental results and revised paleotemperature equations. Paleoceanography 13, 150–160.

Boyle, E.A., 1988. Cadmium: chemical tracer deep water paleoceanography. Paleoceanography 3, 471–489.

Chappell, J., Polach, H., 1991. Post-glacial sea-level rise from a coral record at Huon Peninsula, Papua New Guinea. Nature 349, 147–149.

Chappell, J., Shackleton, N.J., 1986. Oxygen isotopes and sea level. Nature 324, 137–140.

Chappell, J., Omura, A., Ezat, T., McCulloch, M., Pandolfi, J., Ota, Y., Pillans, B., 1996. Reconciliation of late Quaternary sea levels derived from coral terraces at Huon Peninsula with deep-sea oxygen isotope records. Earth and Planetary Science Letters 141, 227–236.

Clarke, G.K.C., Marshall, S.J., 2002. Isotopic balance of the Greenland Ice Sheet: modelled concentrations of water isotopes from 30,000 BP to present. Quaternary Science Reviews 21 (1–3), this issue.

Coplen, T.B., 1988. Normalization of oxygen and hydrogen isotope data. Chemical Geology 72, 293–297.

Cortijo, E., Duplessy, J.C., Labeyrie, L., Leclaire, H., Duprat, J., van Weering, T.C.E., 1994. Eemian cooling in the Norwegian Sea and North Atlantic Ocean preceding continental ice-sheet growth. Nature 372, 446–449.

Cortijo, E., Lehman, S., Keigwin, L.D., Chapman, M., Paillard, D., Labeyrie, L., 1999. Changes in meridional temperature and salinity

gradients in the North Atlantic Ocean (32° to 72°N) during the last interglacial period. Paleoceanography 14, 23–33.

Curry, W.B., Duplessy, J.C., Labeyrie, L.D., Shackleton, N.J., 1988. Changes in the distribution of $\delta^{13}C$ of deep water ΣCO_2 between the Last Glaciation and the Holocene. Paleoceanography 3, 317–341.

Delaygue, G., Masson, V., Jouzel, J., Koster, R.D., Healy, R.J., 2000. The origin of Antarctic precipitation: a modelling approach. Tellus 52B, 19–36.

Duplessy, J.-C., Moyes, J., Pujol, C., 1980. Deep water formation in the North Atlantic Ocean during the last ice age. Nature 286, 479–482.

Duplessy, J.-C., Shackleton, N.J., Matthews, R.K., Prell, W., Ruddiman, W.F., Caralp, M., Hendy, C.H., 1984. ^{13}C record benthic foraminifera in the last interglacial ocean: implications for the carbon cycle and the global deep water circulation. Quaternary Research 21, 225–243.

Duplessy, J.-C., Shackleton, N.J., Fairbanks, R.G., Labeyrie, L., Oppo, D., Kallel, N., 1988a. Deep water source variations during the last climatic cycle and their impact on the global deep water circulation. Paleoceanography 3, 343–360.

Duplessy, J.C., Labeyrie, L., Blanc, P.L., 1988b. Norwegian Sea deep water variations over the last climatic cycle: paleo-oceanographical implications. In: Wanner, H., Siegenthaler, U. (Eds.), Long and Short Term Variability of Climate. Springer, Berlin, pp. 83–116.

Duplessy, J.C., Labeyrie, L., Arnold, M., Paterne, M., Duprat, J., van Weering, T.C.E., 1992. Changes in surface salinity of the North Atlantic Ocean during the last deglaciation. Nature 358, 485–487.

Fairbanks, R.G., 1989. A 17 000-year glacio-eustatic sea-level record: influence of glacial melting rates on the younger dryas event and deep ocean circulation. Nature 342, 637–642.

Gallup, C.D., Edwards, R.L., Johnson, R.G., 1994. The timing of high sea levels over the past 200,000 years. Science 263, 796–800.

Hanebuth, T., Stattegger, K., Grootes, P.M., 2000. Rapid flooding of the Sunda Shelf: a late-glacial sea-level record. Science 288, 1033–1035.

Hut, G., 1987. Stable Isotope Reference Samples for Geochemical and Hydrological Investigations. International Atomic Energy Agency, Vienna.

Imbrie, J., Hays, J.D., Martinson, D.G., McIntyre, A., Mix, A.C., Morley, J.J., Pisias, N.G., Prell, W.L., Shackleton, N.J., 1984. The orbital theory of Pleistocene climate: support from a revised chronology of the marine $\delta^{18}O$ record. In: Berger, A., Imbrie, J., Hays, J., Kukla, G., Saltzman, B. (Eds.), Milankovitch and climate. Reidel Publishing Company, Dordrecht, pp. 269–305.

Labeyrie, L.D., Duplessy, J.C., Blanc, P.L., 1987. Variations in mode of formation and temperature of oceanic deep waters over the past 125 000 years. Nature 327, 477–482.

Lambeck, K., Chappell, J., 2001. Sea level change through the last glacial cycle. Science 292, 679–686.

Lambeck, K., Yokoyama, Y., Purcell, T., 2002. Into and out of the Last Glacial Maximum: sea-level change during oxygen isotope stages 3 and 2. QSR. Quaternary Science Reviews 21 (1–3), this issue.

Lemoine, F., 1998. Changements de l'hydrologie de surface de l'Océan Austral en relation avec les variations de la circulation thermohaline au cours des deux derniers cycles climatiques. Thèse de doctorat, Université Paris, Vol. VI. 175pp.

Levitus, S., 1994. World Ocean Atlas. NOAA, Washington, DC.

Lorius, C., Merlivat, L., 1977. Distribution of mean surface stable isotope values in East Antarctica. Observed changes with depth in a coastal area. In: IAHS (Eds.), Vienna, IAHS, pp. 125–137.

Lynch-Stieglitz, J., Curry, W.B., Slowey, N., 1999. A geostrophic transport estimate for the Florida current from the oxygen isotope composition of benthic foraminifera. Paleoceanography 14, 360–373.

Martinson, D.G., Pisias, N.G., Hays, J.D., Imbrie, J., Moore, T.C., Shackleton, N.J., 1987. Age dating and the orbital theory of the ice ages: development of a high-resolution 0 to 300 000 year chronostratigraphy. Quaternary Research 27, 1–29.

McManus, J.F., Oppo, D.W., Cullen, J.L., 1999a. Glacial modulation of rapid climate change during the last 0.5 million years. PAGES Newsletter 7 (3), 12–513.

McManus, J.F., Oppo, D.W., Cullen, J.L., 1999b. A 0.5-million-year record of millenial-scale climate variability in the North Atlantic. Science 283, 971–975.

Mix, A.C., Ruddiman, W.F., 1984. Oxygen-isotope analyses and Pleistocene ice volumes. Quaternary Research 21, 1–20.

Ostlund, H.G., Craig, H., Broecker, W.S., Spencer, D., 1987. GEOSECS Atlantic, Pacific and Indian ocean expeditions, shorebased data and graphics, Vol. 7. Technical report, I.D.O.E. National Science Fundation, p. 200.

Paillard, D., Labeyrie, L., Yiou, P., 1996. Macintosh program performs time-series analysis. EOS 77, 379.

Rohling, E.J., Bigg, G.R., 1998. Paleosalinity and $\delta^{18}O$: a critical assessment. Journal of Geophysical Research 103 (C1), 1307–1318.

Rohling, E.J., Fenton, M., Jorissen, F.J., Bertrand, P., Ganssen, G., Caulet, J.-P., 1998. Magnitudes of sea-level lowstands of the past 500,000 years. Nature 394, 162–165.

Salvignac, M.E., 1998. Variabilité hydrologique et climatique dans l'Océan Austral au cours du Quaternaire terminal. Thèse de doctorat, Université de Bordeaux I, 354pp.

Sarnthein, M., Winn, K., Jung, S.J.A., Duplessy, J.C., Labeyrie, L., Erlenkeuser, H., Ganssen, G., 1994. Changes in east Atlantic deep water circulation over the last 30 000 years: eight time slice reconstructions. Paleoceanography 9, 209–267.

Schrag, D.P., Hampt, G., Murray, D.W., 1996. Pore fluid constraints on the temperature and oxygen isotopic composition of the glacial ocean. Science 272, 1930–1932.

Shackleton, N.J., 1974. Attainment of isotopic equilibrium between ocean water and benthonic foraminifera genus *Uvigerina*: isotopic changes in the ocean during the last glacial. Les méthodes quantitatives d'étude des variations du climat au cours du Pleistocène, Gif-sur-Yvette. Colloque international du CNRS 219, 203–210.

Shackleton, N.J., 1987. Oxygen isotopes, ice volume and sea level. Quaternary Science Reviews 6, 183–190.

Shackleton, N.J., 2000. The 100,000-year Ice-Age cycle identified and found to lag temperature, carbon dioxide, and orbital eccentricity. Science 289, 1897–1902.

Shackleton, N.J., Pisias, N.G., 1985. Atmospheric carbon dioxide, orbital forcing, and climate. In: Sundquist, E., Broecker, W.S. (Eds.), The Carbon Cycle and Atmospheric CO_2: Natural Variations Archean to Present. AGU, Washington, D.C, pp. 303–317.

Shackleton, N.J., Imbrie, J., Hall, M.A., 1983. Oxygen and carbon isotope record of East Pacific core V 19-30: implications for deep water in the late Pleistocene North Atlantic. Earth and Planetary Science Letters 65, 233–244.

Shackleton, N.J., Berger, A., Peltier, W.R., 1990. An alternative astronomical calibration of the lower Pleistocene timescale based on ODP Site 677. Transactions of the Royal Society of Edinburgh: Earth Sciences 81, 251–261.

Sowers, T., Bender, M., Labeyrie, L., Martinson, D., Jouzel, J., Raynaud, D., Pichon, J.J., Korotkevich, Y.S., 1993. A 135000-year Vostok-Specmap common temporal framework. Paleoceanography 8, 737–766.

Stein, M., Wasserburg, G.J., Aharon, P., Chen, J.H., Zhu, Z.R., Bloom, A., Chappell, J., 1993. TIMS U-series dating and stable isotopes of the last interglacial event in Papua New Guinea. Geochemica et Cosmochemica Acta 57, 2541–2554.

Stirling, C.H., Esat, T.M., McCulloch, M.T., Lambeck, K., 1995. High-precision U-series dating of corals from Western Australia and implications for the timing and duration

of the Last Interglacial. Earth and Planetary Science Letters 135, 115–130.

Stuiver, M., Reimer, P.J., Bard, E., Beck, J.W., Burr, G.S., Hughen, K.A., Kromer, B., McCormac, G., Van Der Plicht, J., Spurk, M., 1998. IN TCAL98 radiocarbon age calibration, 24,000-0 cal BP. Radiocarbon 40, 1041–1083.

Vidal, L., Labeyrie, L., Cortijo, E., Arnold, M., Duplessy, J.C., Michel, E., Becqué, S., van Weering, T.C.E., 1997. Evidence for changes in the North Atlantic Deep Water linked to meltwater surges during the Heinrich events. Earth and Planetary Science Letters 146, 13–26.

Waelbroeck, C., Duplessy, J.C., Michel, E., Labeyrie, L., Paillard, D., Duprat, J., 2001. The timing of the last deglaciation in North Atlantic climate records. Nature 412, 724–727.

Yokoyama, Y., Lambeck, K., De Deckker, P.P.J., Fifield, L.K., 2000. Timing of the last glacial maximum from observed sea-level minima. Nature 406, 713–716.

Zhu, Z.R., Wyrwoll, K.H., Collins, L.B., Chen, J.H., Wasserburg, G.J., Eisenhauer, A., 1993. High-precision U-series dating of Last Interglacial events by mass spectrometry: Houtman Abrolhos Islands, Western Australia. Earth and Planetary Science Letters 118, 281–293.